Reactive Coupling between Immiscible Polymer Chains: Acceleration by Compressive Flow

Jie Song, Adam M. Baker, and Christopher W. Macosko
Dept. of Chemical Engineering and Materials Science, University of Minnesota, Minneapolis, MN 55455

Randy H. Ewoldt
Dept. of Chemical Engineering and Materials Science, University of Minnesota, Minneapolis, MN 55455

The Institute for Mathematics and its Applications, University of Minnesota, Minneapolis, MN 55455

DOI 10.1002/aic.14092
Published online May 1, 2013 in Wiley Online Library (wileyonlinelibrary.com)

It is demonstrated that processing flow affects the kinetics of the interfacial coupling reaction between functional groups that are grafted to polymer chains. At melt temperatures the amine group on the end of nylon 6 chains reacts with maleic anhydride grafted polyethylene (PE-MA) and forms graft copolymers. Bilayers were made by lamination and coextrusion and adhesion was measured using asymmetric dual cantilever beam (ADCB). The amount of graft copolymer in the interface was quantified by X-ray photon spectroscopy (XPS). With quiescent lamination, adhesion increased with temperature and the concentration of PE-MA. The adhesion metric, G_c (critical energy release rate), plotted as a function of Σ (interfacial copolymer density) fell on the same master curve, unifying reaction process, temperature and time. G_c was a linear function of Σ for low-copolymer coverage and weak adhesion. For relatively high coverage and strong adhesion, G_c scaled with Σ^2. Coextrusion with compressive flow resulted in a reaction rate strikingly two-orders of magnitude faster than that without compressive flow. The rate in the noncompressive die was close to quiescent lamination. Even for lamination, when compressive flow was applied normal to the interface, the coupling reaction rate was also greatly accelerated. Several mechanisms are speculated for this remarkable acceleration in polymer chain coupling. © 2013 American Institute of Chemical Engineers *AIChE J*, 59: 3391-3402, 2013
Keywords: reaction kinetics, interfacial processes, rheology, multiphase flow, polymer processing

Introduction

Neal Amundson's influence on the senior author's life began when I read his publications on polymerization modeling[1,2] during my M.Sc. research at Imperial College. The "Chief" changed my life when he walked into my graduate student office at Princeton and encouraged me to also consider an academic career. Becoming the first "polymeric glue" in Minnesota's newly formed Dept. of Chemical Engineering and Materials Science has been wonderfully fulfilling. Amundson did consider reactions in two phases[3] and I believe would have had some insightful comments on our case where reactions are confined to the interface between the phases.

Most polymer pairs are thermodynamically immiscible. As a result, they form two phases upon blending. The interface is weak due to lack of entanglements between both polymers. Coupling reactions between functional group grafted macromolecules have been proven to be a powerful way to stabilize blend morphology and increase adhesion.[4–6] These compatibilized blends can have properties superior to their single component polymers.[7] Premade block copolymers have also been used to compatibilize blends, however, interfacial coupling reactions have advantages: (1) most of the copolymers formed stay at the interface; and (2) coupling reactions can link many homopolymer pairs for which the complementary block copolymer synthesis is not available.[8,9]

Yet the reaction kinetics of interfacial coupling requires more fundamental understanding. Although many aspects of reactive blending have been investigated by using quiescent bilayers including reactivity,[10] architecture,[11] molecular weight,[12] and concentration of functional polymers,[13] reaction kinetics under flow still remains a challenge. The common wisdom for reactions between *small molecules* under flow is that external mass transfer increases the reaction rate by increasing concentration of reactive species without affecting reaction mechanism and transition states at a certain temperature. However, for reactions between *macromolecules* under flow, the kinetics is more complicated. It is generally difficult to study the effects of flow on macromolecular reactions, especially difficult for polymers during mixing, because interfacial area generation and flow patterns are always convoluted and hard to isolate.

Coextrusion is widely used to produce multilayer sheets.[14–18] It is a process in which two or more polymer layers are combined and extruded simultaneously. As the interface is well defined, coextrusion provides an ideal model

Correspondence concerning this article should be addressed to J. Song at songx114@umn.edu.

Current address of Randy H. Ewoldt: Dept. of Mechanical Science and Engineering, University of Illinois at Urbana-Champaign, Champaign, IL 61801

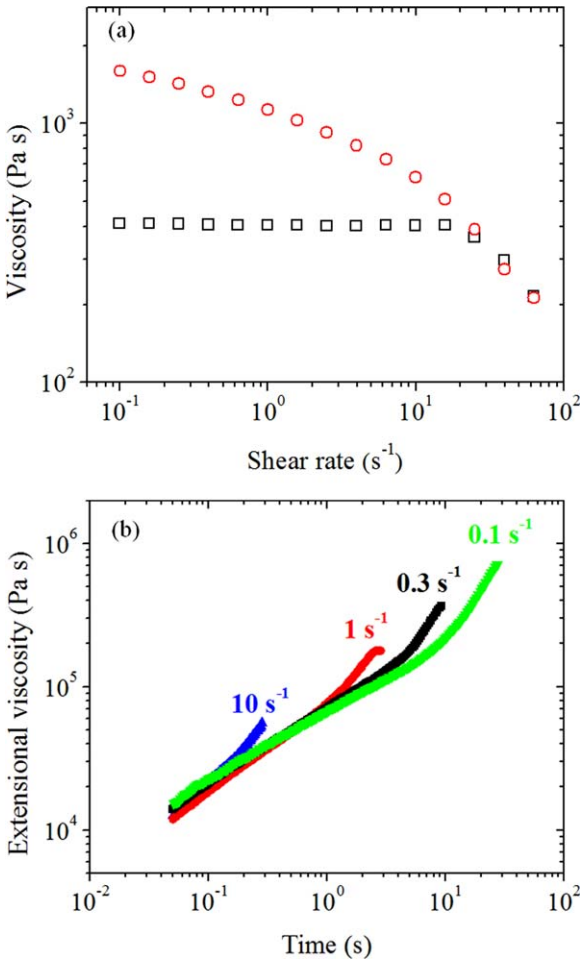

Figure 1. (a) Steady-shear viscosity vs. shear rate at 230°C. □: nylon 6; ○: PE-MA, (b) transient uniaxial extensional viscosity of PE-MA at 150°C at several extension rates.

[Color figure can be viewed in the online issue, which is available at wileyonlinelibrary.com.]

system for studying interfacial phenomena such as interdiffusion,[19] reaction,[20] and slip at polymer–polymer interfaces.[18,21] However, few studies have investigated how the interfacial reaction and adhesion depend on the flow conditions during processing.

Jeon et al.[22] found that with complex mixing flows, interfacial reactions were accelerated compared with simple lamination. Zhang et al.[20] determined that the coupling reaction of amine terminal polystyrene/anhydride terminal poly(methyl methacrylate) in coextrusion, in the absence of mixing, was up to 1000 times faster than that under quiescent annealing. Yet shear flow was convoluted with compressive/extensional flow at the interface in their multilayer coextrusion.

In our recent research we further simplified flow patterns and eliminated shear flow by using bilayer coextrusion.[5] We determined that the coupling reaction rate between functional polyethylenes and the urethane groups in thermoplastic polyurethane was about one order of magnitude faster than lamination.

In this article, we will show that *compressive flow alone* can accelerate coupling reactions dramatically. Here we study a different chemistry, i.e., the reaction between PE-MA (maleic anhydride grafted polyethylene) and the terminal amine groups on nylon 6. This allowed us to quantify nylon graft density and thus reaction conversion directly rather than indirectly via the increase in adhesion. Compared to lamination, compressive flow gave rise to two orders of magnitude reaction acceleration.

Experimental

Materials

Low-viscosity general-purpose, extrusion grade nylon 6 (Ultramid B 27) was provided by BASF. It has a density of 1.13 g/cm^3, melt flow rate of 130 cc/10 min (275°C/5 Kg), melting point of 220°C, Mn of 17 kg/mol and PDI of 2.0. This nylon 6 has nominally one NH_2 group at the end of each chain according to the manufacturer. All the data came from the material provider. Formic acid and trifluoroacetic acid (Sigma-Aldrich) were used as received.

PE-MA was provided by Chemtura Co. with trade name Polybond 3029. It has a density of 0.96 g/cm^3, melt flow rate of 4 g/10 min (190°C/2.16 Kg), melting point of 130°C, Mn of 13 kg/mol and PDI of 5.8. The MA content is 1.6 wt %. PE-MA was blended into high-density polyethylene (Dow HDPE 25455N) to study the effect of PE-MA concentration on adhesion. This HDPE has a density of 0.957 g/cm^3 and melting point of 129°C. Nylon 6 and PE-MA pellets were dried overnight in a conventional static oven at approximately 70°C to remove residual moisture before compression molding and coextrusion. The viscosities were measured under N_2 atmosphere by a strain controlled rotational rheometer (ARES, TA Instruments) using 25 mm parallel plates at 230°C for shear and the EVF fixture at 150°C for uniaxial extension. Figure 1a shows that steady-shear viscosity values at 230°C for nylon 6 and PE-MA were similar, within ±30%, over the rate range 10–60 s^{-1}, the range of wall shear rates in the dies. Figure 1b shows the extensional viscosity data for PE-MA; 150°C was used to reduce sagging during the experiment. Figure 2 gives the dynamic frequency sweep of PE-MA at 230°C. Generalized Maxwell model was used to fit the data.[23]

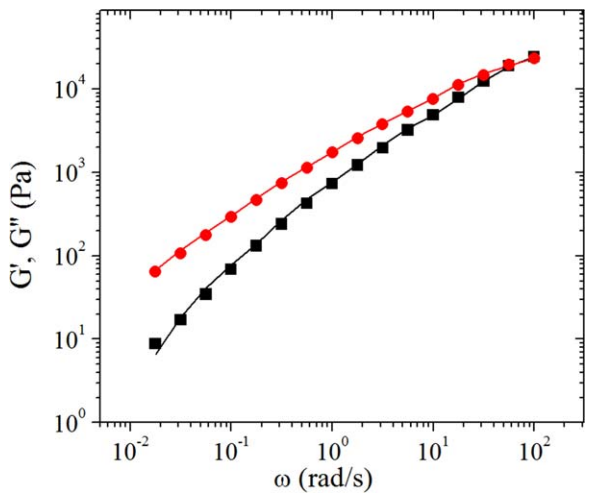

Figure 2. Dynamic frequency sweep of PE-MA at 230°C. ■: G′; ●: G″.

Solid lines represent generalized Maxwell model fitting. [Color figure can be viewed in the online issue, which is available at wileyonlinelibrary.com.]

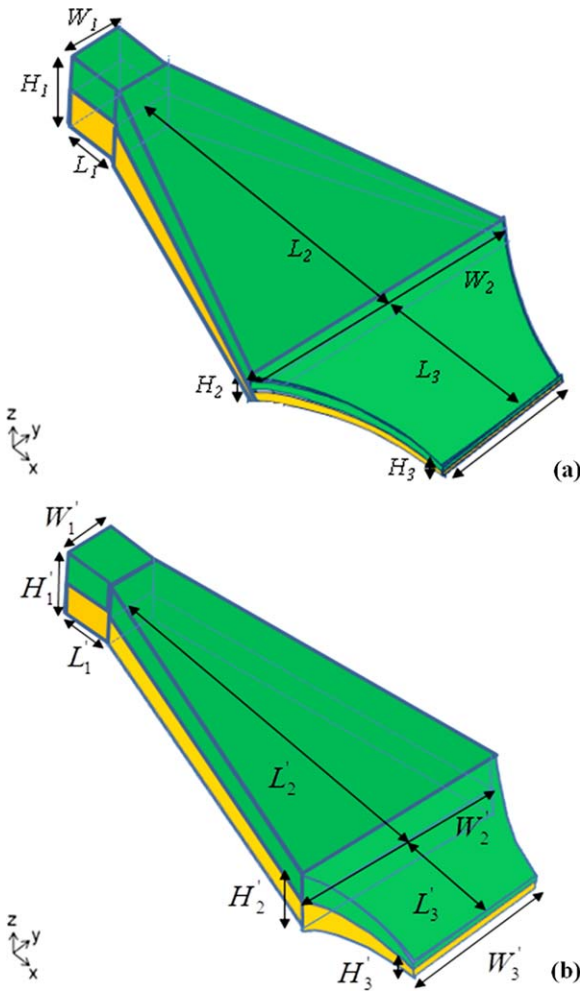

Figure 3. Schematic of polymer flow inside coextrusion dies and upon exiting the dies.

(a) Compressive die, and (b) noncompressive die. In figure (a), $H_1 = 12.5$ mm, $W_1 = 12.5$ mm, $L_1 = 14.2$ mm, $H_2 = 1.2$ mm, $W_2 = 50$ mm, $L_2 = 33.5$ mm. In (b), $H_1' = H_2' = 12.5$ mm (no compression), $W_2' = 40$ mm, $L_2' = 50$ mm, with all the other dimensions being the same as the compressive die. H_3 and H_3' were controlled by the take-up rolls as discussed in the text. L_3 and L_3' were held at 85 mm. [Color figure can be viewed in the online issue, which is available at wileyonlinelibrary.com.]

Coextrusion and lamination

The PE-MA and nylon 6 bilayer samples were prepared by coextrusion at 230°C through dies shown schematically in Figure 3. In the compressive die, the interfacial plane experiences dilation (increased area) which in general requires extension in at least one direction. The compressive die used here causes extension in both the *y*- and *x*-direction, dominated by the *x*-direction extension (see Appendix and Figure 12 for a discussion on kinematics.). In the noncompressive die, there was no compressive flow since the thickness of the die was kept constant. Polymer melts were delivered by single-screw extruders to a gear pump (Zenith PEP-II), which controlled the flow rate to the feedblock. Two polymers were extruded at equal flow rate. A detailed description of the coextrusion line can be found in the literature.[20,21,24,25] Based on the continuity equation, melt velocity in the coextrusion dies can be deduced from the chill roll speed and film thickness. At a total flow rate of 33.6 cm^3/min determined from calibrated gear pumps, the average linear velocity of the polymer melt at the die exit was about 10 mm/s. Thus, the residence time in the sheeting die was less than 10 s. On exiting the die, bilayer films were drawn by chill rolls whose temperature was set at 4°C. The length of the air gap L_3, was held at 85 mm and chill roll speed was varied between 64 cm/min and 185 cm/min to obtain different reaction times. Increasing roll speed reduced residence time and decreased thickness of the bilayer samples. Samples from the compressive die were drawn down from 1.2 mm to 1.14–0.49 mm depending on the chill roll speed, while samples from the noncompressive die were drawn down from 12.5 mm to 3.0–1.2 mm. The surface temperature of molten polymer in the air gap was measured by an infrared thermometer (Omega Engineering, Inc.) and found to decrease from 230°C by no more than 4°C for all the extrusions. As described later adhesion tests on coextruded films were conducted after 24 h.

PE-MA/HDPE and nylon sheets (80 mm × 7.5 mm × 0.4 mm) were prepared from pellets by compression molding at 180°C and 230°C, respectively in a hydraulic press under 2 MPa between two polytetrafluoroethylene (PTFE) coated aluminum foils (Saint-Gobain Performance Plastics). PE-MA/HDPE and nylon sheets were dried *in vacuo* at 80°C and then pressed into intimate contact very gently (~0.1 MPa), and annealed for various times at 230°C within a steel rectangular mold (80 mm × 7.5 mm × 0.75 mm). Immediately after annealing, bilayer samples were quenched by plunging into ice water. The edges of bilayer samples were trimmed with a razor blade before adhesion tests.

To generate more compressive flow during melt lamination, a pair of thicker layers (0.6 mm instead of 0.4 mm) was compressed under 2 MPa from 1.2 mm down to 0.84, 0.6, 0.45, 0.36 and 0.19 mm using different thickness molds to test the change of adhesion with various compressive strains. After the initial fast squeezing, <1 s, the bilayers were annealed for 10 s at 230°C.

Characterization

Adhesion Measurement by ADCB (Asymmetric Dual Cantilever Beam) Test. The ADCB test has been shown to be a reliable method to determine the adhesion strength between stiff polymers and been used to quantify the effect of adding block copolymers.[26] The edges of annealed bilayer samples were trimmed before adhesion measurement. A rectangular blade was inserted into the interface of a bilayer sample to initiate a crack. After allowing the crack to equilibrate for 24 h, the crack length a, was measured from the crack front to the tip of the wedge. An optical microscope was used for measuring short crack length. Three to five replicates were measured for each data point.

The driving force for the propagation of crack comes primarily from the stiffness of the beams separated by the wedge and this driving force decreases as the crack propagates. The crack stops propagation when the release rate of elastic energy equals the energy needed to create a unit surface.

The critical rate of energy release has to be calculated in the proper limit. Since the crack length ahead of the blade *a*, was less than 10 times the layer thickness, h,for most of our samples, the following equation derived by Boucher et al.[27] was used. Kanninen[28] assumed that the finite elasticity of the material ahead of the crack tip required correction for small crack length which was extended to describe ADCB test.

The critical fracture toughness or critical strain energy release rate (G_c) can be calculated using Eq. 1 as follows[27]

$$G_c = \frac{3\Delta^2}{8a^4} \frac{E_{PE-MA} E_{Nylon} h_{PE-MA}^3 h_{Nylon}^3}{E_{PE-MA} h_{PE-MA}^3 \alpha_{Nylon}^2 + E_{Nylon} h_{Nylon}^3 \alpha_{PE-MA}^2} \quad (1)$$

where $\alpha_i = \left(1 + 1.92\frac{h_i}{a} + 1.22\left(\frac{h_i}{a}\right)^2 + 0.39\left(\frac{h_i}{a}\right)^3\right) / \left(1 + 0.64\frac{h_i}{a}\right)$, Δ is the thickness of the razor blade, E_i is the modulus of component i, and h_i is the thickness of the component i. ($i = 1$, 2) The modulus and thickness of each layer, as well as the crack length, are required for the calculation of the critical mechanical energy release rate.

X-ray Photoelectron Spectroscopy (XPS) Determination of interfacial copolymer density Σ. To determine the amount of copolymers formed at the interface, we used the method developed by Boucher et al.[29] The same nylon 6/PE-MA bilayer samples on which G_c had been previously measured were used. To remove the bulk nylon and keep the graft copolymer chains in place, samples were put into a formic acid bath for at least 24 h at room temperature. Although formic acid is a good solvent for nylon, free chains of nylon were linked by hydrogen bonds to the copolymer chains. In order to remove these free chains, the formic acid washed PE-MA bulk samples were subsequently treated with trifluoroacetic anhydride in the gas phase to break the hydrogen bonding. The treated samples were then washed with dichloromethane to remove the free chains. Deionized water was then used to detach the trifluoroacetyl functional groups. Finally the treated samples were put into vacuum oven at room temperature with their fresh surfaces upward and covered carefully to prevent contamination. They were analyzed within 1 day to minimize contamination and oxidation of the grafted chains.

XPS measurements were performed on a Surface Science SSX-100 spectrometer using a focused monochromatic Al Ka anode (hv = 1486.6 eV) and a spot size of 800 μm. Electrostatic charging was neutralized by mounting a nickel grid about 2 mm above the sample surfaces. An accelerating voltage of 10 kV was used for data acquisition. After reflections corresponding to binding energies of C_{1s}, O_{1s} and N_{1s} were identified, higher resolution spectra were recorded for elemental quantification. The recorded spectra were adjusted to the C_{1s} peak of the saturated hydrocarbon bonds at a binding energy 286 eV. The elemental compositions were quantified from the peak areas using Wagner's sensitivity factors [30] and the spectrometer transmission function was taken into account. The parameters used for fitting were the peak area, the peak full width at half maximum, the position of the peak maximum, and the Gaussian-Lorentzian ratio. The copolymer surface density Σ can be calculated from the XPS intensities of carbon and nitrogen as

$$\Sigma = -\frac{N_a \rho \lambda \sin\theta}{M_n} \ln\left(1 - \frac{I_N/I_C}{I_N^\infty/I_C^\infty}\right) \quad (2)$$

where N_a is Avogadro's number, ρ the density of nylon 6, M_n the number-average molar mass of nylon 6, λ the mean free path of N_{1s} photoelectrons, and θ the takeoff angle. The escape length of the photoelectrons, $\lambda \sin\theta$, was estimated to be 19 Å using an experimentally determined relationship for escape length through hydrocarbon layers.[31] I_C and I_N are the intensities of the carbon and nitrogen peaks on the analyzed sample surface and I_C^∞ and I_N^∞ are the intensities of these peaks on a pure nylon 6 surface. The ratio of I_C^∞ over I_N^∞ equals 6/1 according the chemical structure of nylon 6.

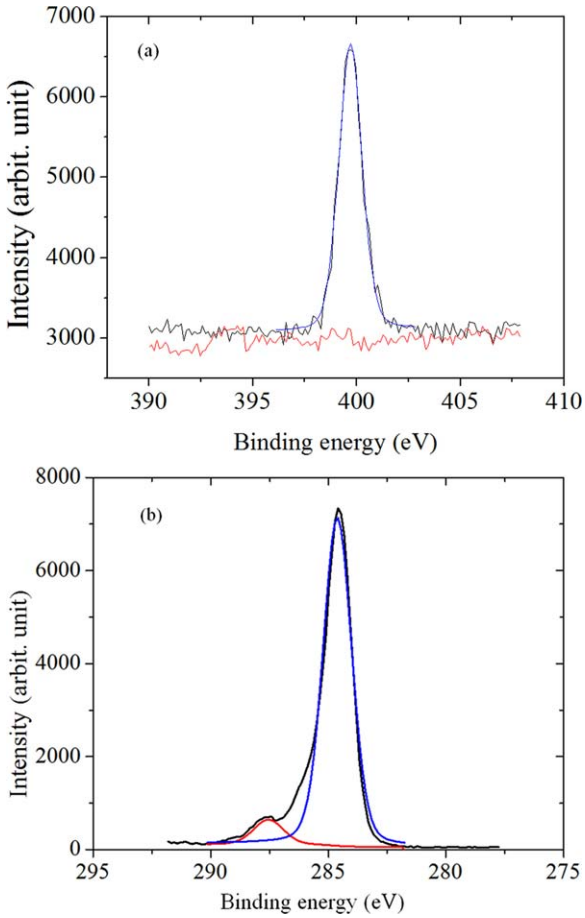

Figure 4. High-resolution XPS spectra of the PE-MA surface after removing free nylon 6 following interfacial reaction. PE-MA was obtained from coextrusion through the compressive die with 12 s reaction time.

(a) Nitrogen (399.6 eV peak). The noisy red line in (a) was HDPE after the same experiment, (b) carbon (284.6 eV peak) with an asymmetric shoulder due to C═O in the nylon backbone. In both (a) and (b) the black curves are original data; blue (and also in (b) red) curves represent deconvolution of the spectrum after curve fitting. [Color figure can be viewed in the online issue, which is available at wileyonlinelibrary.com.]

We measured copolymer areal density Σ by XPS for each sample. Figure 4 shows typical XPS spectra of the PE-MA surface after removing undreacted nylon 6. Figure 4a exhibits a symmetric N_{1s} peak centered at 399.6 eV. For the grafted nylon chains, there are two different kinds of N: the one next to carbonyl in the original nylon backbones and the one in the imide group after reaction. Due to the low concentration of the N in imide, XPS shows only the first type. An asymmetric C_{1s} peak centered at 284.6 eV has a shoulder toward higher binding energy, indicating the presence of C═O in the nylon backbone.

Scanning Electron Microscopy (SEM). SEM images were taken with a JEOL 6500 scanning electron microscope with a field-emission gun on cleaved surfaces after adhesion tests. SEM samples were sputter-coated with platinum to a thickness of approximately 75 angstroms to make them conductive. Electron beam current and potential were varied for optimal imaging.

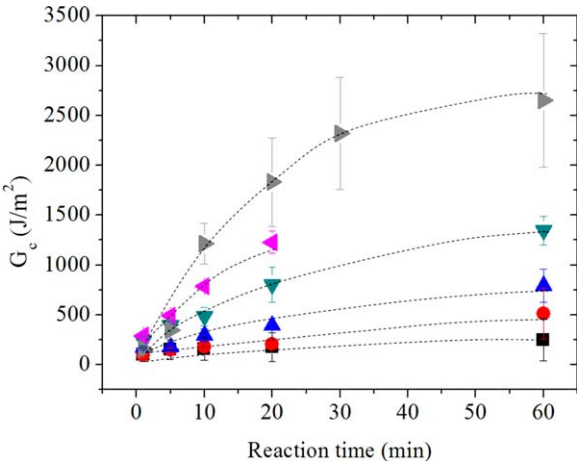

Figure 5. Critical energy release rate G_c development as a function of reaction time for adhesion between laminated nylon 6 and PE-MA/HDPE blends at 230°C.

Concentration of PE-MA in the blends indicated by ▶: 100 wt %, ◀: 80 wt %, ▼: 50 wt %, ▲: 20 wt %, ●: 10 wt %, ■: 5 wt %. Dashed lines are used to guide the eye. [Color figure can be viewed in the online issue, which is available at wileyonlinelibrary.com.]

Results and Discussion

The development of Σ and G_c and their correlations

The dependence of adhesion energy G_c, vs. the reaction time t for quiescently laminated nylon 6/PE-MA joints prepared at 230°C is reported in Figure 5. G_c increases with the reaction time as well as the concentration of PE-MA, C_o, as shown in Figure 6. For this system the adhesion can be predictably controlled through the concentration of PE-MA blended into the HDPE matrix.

The XPS results in Figure 4 demonstrate that graft copolymer molecules were indeed formed at the interface. Their areal densities Σ, are plotted in Figure 7 as a function of reaction time and temperature for lamination between nylon

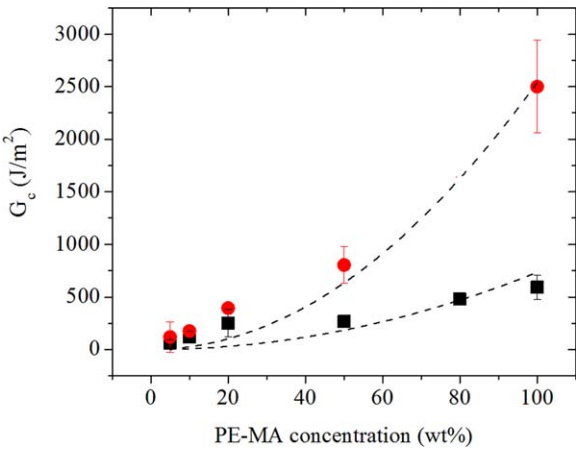

Figure 6. Critical energy release rate G_c development as a function of C_0, PE-MA concentration, for lamination at 170 and 230°C with reaction time 60 min ■: 170°C, ●: 230°C. The broken lines are power law fitting of the data with an exponent of 2.

[Color figure can be viewed in the online issue, which is available at wileyonlinelibrary.com.]

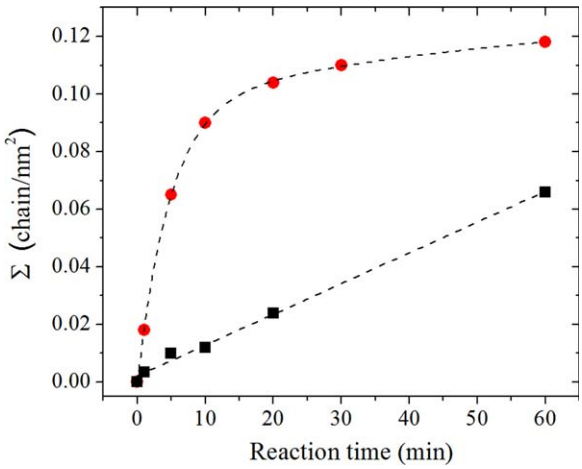

Figure 7. Interfacial copolymer density Σ vs. reaction time for lamination between nylon 6 and PE-MA.

■:170°C; ●:230°C. At 170°C Σ increases linearly with reaction time. The dashed line for 230°C is to guide the eye. [Color figure can be viewed in the online issue, which is available at wileyonlinelibrary.com.]

6 and PE-MA. Σ built-up much faster at 230°C in contrast to 170°C. At 170°C, Σ shows a linear development with reaction time t, indicating a constant reaction rate at the initial stage of the coupling reaction.

Table 1 summarizes the development of G_c and Σ as a function of process type, temperature and reaction time. By cross plotting the data from Table 1, the resulting dependence of G_c as a function of Σ is shown in Figure 8. It is quite remarkable that all the data for samples made at different temperatures and time (and even lamination and coextrusion) fall approximately on the same master curve. The measured critical energy release rate of the interface scaled as $G_c \propto \Sigma^2$ for high Σ coverage and scaled as $G_c \propto \Sigma$ for relatively low coverage. Combining the relationship in Figure 6 with the data in Figure 7, we have $\Sigma \propto C_0$, indicating the reaction rate is proportional to the concentration of reactive species at the initial stage of reaction.

G_c, the work required to produce a unit increase in crack area, is a linear function of Σ if the interface failure occurs by simple chain scission or chain pull-out without any extensive plastic deformation. It scales with Σ^2 if the applied interfacial stress is sufficient to activate plastic deformation of a small volume at the crack tip.[32,33] Those failure mechanisms apply to glassy polymers. However, semicrystalline polymers are also of interest, raising the question of whether the same models can be applied. Brown derived an equation that describes the behavior of glassy and semicrystalline polymers when the main plastic deformation mechanism ahead of the crack tip is a craze and when failure of the craze occurs by chain scission in the fibrils. He showed that for adhesion between glassy polymers[34]

$$G_c \approx \frac{\Sigma^2 f_b^2 2\pi D}{\sigma_d}\left(\frac{S_{22}}{S_{12}}\right)\left(1-\frac{1}{\lambda}\right) \tag{3}$$

where D is the craze fibril diameter, f_b is the force needed to break a covalent bond, σ_d is the crazing stress, and λ is the fibril extension ratio. S_{22} and S_{12} are the tensile and shear compliances of the crazed material, respectively. According to Eq. 3, G_c scales as Σ^2 when all the other parameters are kept the same.

Table 1. Σ and G_c Development for the Coupling Reaction of PE-MA and Nylon 6

Process	Temperature (∘C)	Reaction time (min)	Σ (chain/nm^2)	G_c (J/m^2)
Lamination[a]	230	1	0.025	157 ± 20.5
Lamination	230	5	0.065	528 ± 159
Lamination	230	10	0.09	1214 ± 203
Lamination	230	20	0.104	1832 ± 443
Lamination	230	30	0.113	2220 ± 560
Lamination	230	60	0.118	2409 ± 662
Lamination[a]	170	1	0.005	8 ± 1
Lamination	170	5	0.007	14 ± 2
Lamination	170	10	0.011	23 ± 4
Lamination	170	20	0.019	119 ± 21
Lamination	170	60	0.063	372 ± 48
Lamination[b]	230	10	0.042	114 ± 21
Lamination[c]	230	10	0.051	206 ± 38
Lamination[d](−0.36)	230	0.17	-	120 ± 20
Lamination(−0.69)	230	0.17	-	210 ± 42
Lamination(−0.98)	230	0.17	-	453 ± 69
Lamination(−1.2)	230	0.17	-	955 ± 109
Lamination(−1.84)	230	0.17	-	1598 ± 230
Coextrusion(C)[e]	230	0.09	0.076	585 ± 143
Coextrusion(C)	230	0.13	0.085	799 ± 139
Coextrusion(C)	230	0.15	0.09	1050 ± 215
Coextrusion(C)	230	0.17	0.115	1500 ± 302
Coextrusion(C)	230	0.2	0.121	2047 ± 224
Coextrusion(C)	230	0.23	0.124	2390 ± 457
Coextrusion(NC)[f]	230	0.17	0.0011	1 ± 0.9
Coextrusion(NC)	230	0.2	0.0018	2 ± 1
Coextrusion(NC)	230	0.23	0.003	4 ± 1
Coextrusion(NC)	230	0.27	0.004	5 ± 1

[a]Lamination with 100% PE-MA
[b]Lamination with PE-MA/HDPE (5/95) blend;
[c]Lamination with PE-MA/HDPE (10/90) blend;
[d]Lamination with 100% PE-MA under different compressive strains $\varepsilon_{zz} = \ln\left(H_f/H_0\right)$ (strain in the parentheses).
[e]Coextrusion with the compressive die;
[f]Coextrusion with the noncompressive die.

This model has been used to predict the adhesion development in glassy polymers with interfacial copolymers. However, the size of fibrils in semicrystalline polymers is on the order of microns, while it is typically about 10 nm for glassy polymers. This size difference may invalidate Brown's continuum model, and overpredict G_c relative to a discrete modeling of the fibrillar structure proposed by Sha et al.[35] for small energies of adhesion. However, the two models are in good agreement for

$$\left(\frac{\sigma_y}{\sum f_b}\right)^2 < 1 \tag{4}$$

Using the value for PE-MA ($\sigma_y = 20$ MPa and $f_b \approx 2 \times 10^{-9}$ N), Eq. 4 predicts a lower limit of $\Sigma = 0.009$ nm^{-2}. Therefore, since the majority of values of Σ in this study were greater than this limit, there is good agreement with the Brown model as shown in Figure 8. Thus, for both glassy and many semicrystalline materials, the adhesion is expected to scale with the square of the areal density of copolymer. As a result, the measured critical energy release rate of the interface scaled as $G_c \propto \Sigma^2$ regardless of reaction temperature and time for both lamination and coextrusion.

Reaction acceleration through coextrusion with a compressive die

For coextrusion, we compared the reaction kinetics and adhesion development with different dies in Figure 9. It is striking that the compressive die built-up adhesion and generated interfacial copolymers almost 100 times faster than the noncompressive die, when all the other parameters were kept the same including type of material, flow rate, temperature and cooling conditions.

It should be noted that the reaction time used here is the summation of residence time in the die and also the dwell time in the air gap. Since the melt temperature only decreased by ∼ 4°C from die exit to the nip point, a significant amount of reaction was expected to occur in the air gap. Figure 9a shows that within only 15 s, the interfacial copolymer density of nylon 6 and PE-MA almost reached a plateau when the compressive die was used, while very little copolymer was formed with the noncompressive die. In Figure 10 we plot the variation of Σ with time for both coextrusion and lamination. Once again, the compressive die showed remarkable reaction acceleration at the same temperature.

We calculated the interfacial coupling reaction rate by simply assuming Σ increases linearly with time at the initial stage of reaction, as verified by data in Figure 7. This suggests first-order interfacial kinetics

$$\sum = vt \tag{5}$$

where v is a two-dimensional (2-D) reaction rate, and t is reaction time. Reaction rates are shown in Table 2. The rate with the compressive die is > 80 times than that of lamination, while the rate with the noncompressive coextrusion die is quite similar to the reaction rate with simple lamination at the same temperature.

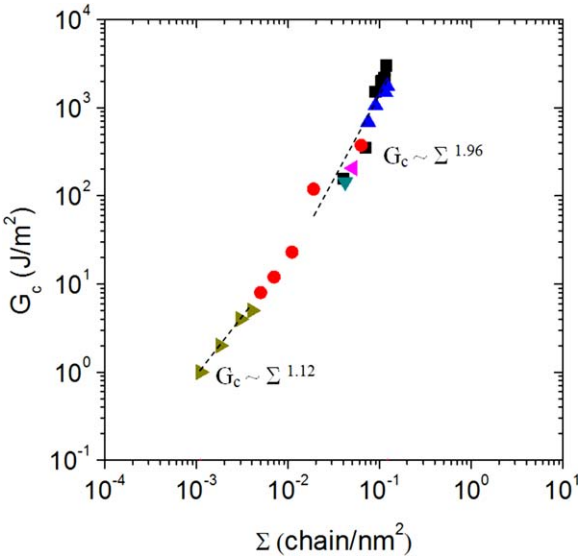

Figure 8. The critical fracture energy G_c directly corresponds to interfacial copolymer density Σ for a variety of processing methods, times and temperatures for nylon 6/PE-MA bilayers.

■: Lamination at 230°C; ▲: Coextrusion at 230°C with compressive die; ▼: Lamination at 230°C, PE-MA/HDPE (5/95); ◀: Lamination at 230°C, PE-MA/HDPE (10/90); ●: Lamination at 170°C; ▶: Coextrusion at 230°C with noncompressive die. The broken lines represent power-law fitting. [Color figure can be viewed in the online issue, which is available at wileyonlinelibrary.com.]

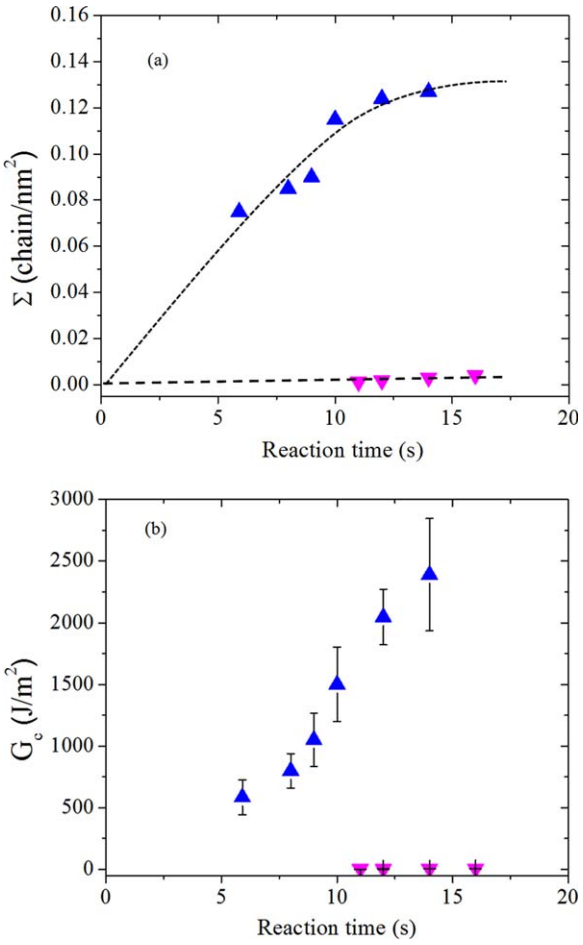

Figure 9. Die comparison for coextrusion of nylon 6 and PE-MA at 230°C; compressive die ▲ vs. noncompressive die ▼.

(a) Σ vs. reaction time, and (b) G_c vs. reaction time. The dashed lines are drawn to guide the eye. [Color figure can be viewed in the online issue, which is available at wileyonlinelibrary.com.]

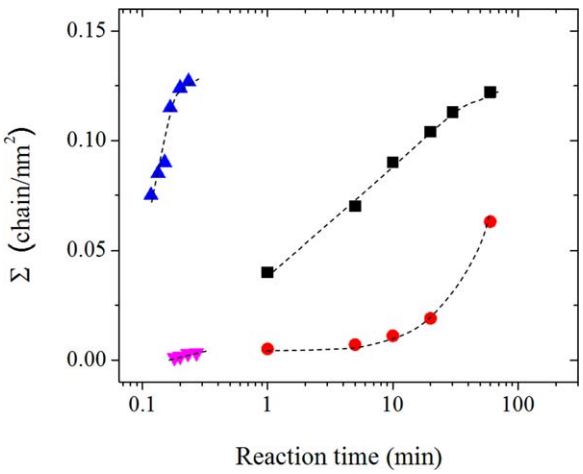

Figure 10. Interfacial copolymer density Σ vs. reaction time for coupling reaction between nylon 6 and PE-MA.

■: lamination at 230°C; ●: lamination at 170°C; ▲: coextrusion with compressive die at 230°C; ▼: coextrusion with noncompressive die at 230°C. The dashed lines are drawn to guide the eye. [Color figure can be viewed in the online issue, which is available at wileyonlinelibrary.com.]

To further compare laminated and coextruded samples the fracture surfaces of the PE-MA/nylon 6 adhesive interface were examined. The SEM images in Figure 11 show distinct difference in the roughness and morphology of cleaved surfaces between strong adhesion in Figure 11a and very weak adhesion in Figure 11b. The fracture surface of nylon bonded via coextrusion at 230°C using the compressive die (11a) with reaction time of only 12 s is similar to the nylon fracture surface (11c) via lamination at 230°C for 30 min. The nylon 6 surface is covered with distorted fibrils and sheets. While strong adhesion gave roughened fracture surfaces, Figure 11b and d showed similar smooth surfaces correlated with weak adhesion. As fewer copolymers were generated at the interface due to short reaction time the interfacial stress during fracture only generated a very small amount of fibrils.

Thus, the Σ quantification by XPS, adhesion measurement and fracture surface images confirm that the interfacial coupling reaction was greatly accelerated by coextrusion using the compressive die in contrast with the noncompressive die and lamination. Next, we will explore the mechanisms that generated this acceleration.

Origin of reaction acceleration

For the coextrusion experiments reported here, reaction acceleration occurs during laminar flow without mixing. Furthermore, the interface is located in the middle of the die, where shear stress approaches zero. However, the interfacial plane does experience compression and extension during coextrusion, as do the bulk phases above and below the interface.

Table 2. Reaction Rates of Interfacial Coupling Reaction Between Nylon 6 and PE-MA

Processing Condition	Reaction rate (chain/(nm^2·min))[a]
Coextrusion (Compressive die, 230°C)	0.86
Coextrusion (Non-compressive die, 230°C)	0.012
Lamination (230°C)	0.011
Lamination (170°C)	0.001

[a]Reaction rate calculated from $\Sigma = vt$.

Under compression/extension conditions, in the absence of shear or mixing, there are several possible causes of the increase of the interfacial reaction rate or the increase of the measured adhesion strength.[5] Although pressure changes the capture volume around a reactive group and accelerates reaction, the pressure dependence of the rate constant for typical liquid-phase reactions is much too weak to alter the rate for the range of pressures encountered here.[36] Crystallinity is known to affect interfacial adhesion,[14,37–39] and this could increase adhesion even with constant copolymer reaction rate. We compared the crystallinity and crystal structures near the interface for coextrusion with different dies. We found that the crystallinity and crystal structures for the same polymer extruded through different dies are almost identical.[25] The stress–strain curves were also the same for films produced by both lamination and coextrusion. Thus, crystallinity plays a negligible role in the observed increase in adhesion strength and we must consider possible mechanisms for increasing the copolymer reaction rate.

We also considered the possibility that compressive flow could modify diffusive flux. We compared the reaction rate to the transport rate by calculating the Damkohler number[5] (the ratio of reaction rate over diffusion rate). We found that compressional flow reduces the diffusion length scale, therefore, increasing the diffusive flux of reactive species to the interface. However, this increase in diffusion is not sufficient to raise the Dampkohler number (10^{-4} to 10^{-3}) from the reaction-limited to the diffusion limited regime (Da $\gg$ 1). We are, therefore, left to conclude that reaction acceleration was mainly caused by an increase in the local reaction process.

Flow-induced orientation is known to accelerate kinetics, e.g., of phase transition with shear-induced crystallization in polymers.[40] It is also known that flow stress and strain can cause polymer chains to break and promote reactions of groups in the polymer backbone.[41] We, therefore, suggest that extensional and compressive flow in the coextrusion process gave rise to the copolymer reaction acceleration observed here.

Sufficiently strong flow can cause polymer chains to orient and extend away from their equilibrium conformations. Flow strength is represented by the Weissenberg number, the ratio of the flow rate to the molecular relaxation rate $Wi = \lambda\dot{\gamma}$. Here λ is the mean relaxation time and $\dot{\gamma}$ is the magnitude of the deformation-rate tensor (see Appendix for definition). Flow-induced chain extension away from equilibrium occurs for $Wi \gtrsim 1$, and this typically results in rheological nonlinearity such a shear-thinning and extensional thickening. We observed shear-thinning in Figure 1a for both nylon 6 (shear

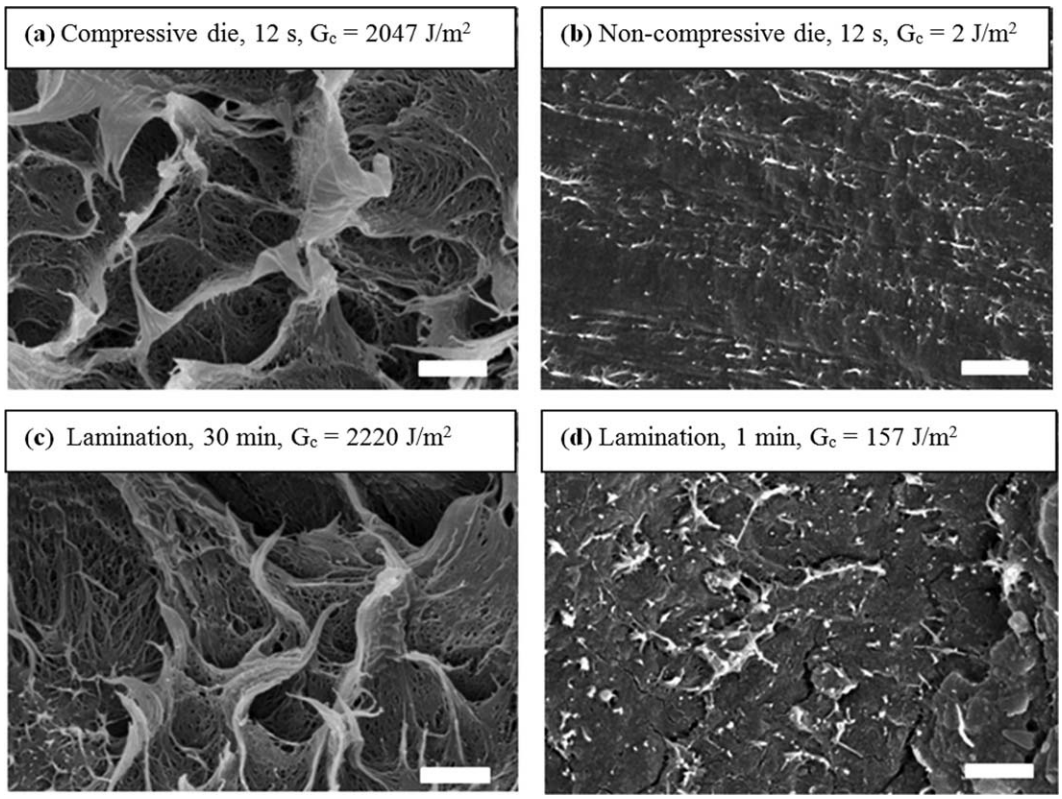

Figure 11. SEM images for cleaved nylon 6 surfaces after adhesion tests.

The PE-MA fracture surfaces were similar. Reaction time and adhesion strength are indicated in each graph. All the scale bars represent 1 μm.

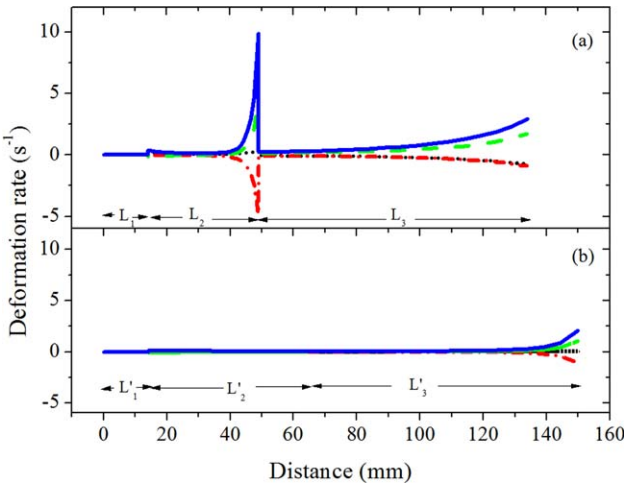

Figure 12. Calculated deformation rate vs. distance for coextrusion at 230°C to demonstrate different degrees of chain extension.

(a) compressive die, and (b) noncompressive die. — · —: $\dot{\varepsilon}_{zz}$ z-direction deformation rate; ···: $\dot{\varepsilon}_{yy}$ y-direction deformation rate; – –: $\dot{\varepsilon}_{xx}$ x-direction deformation rate; ——: $\dot{\gamma}$ square root of the second invariant of deformation rate tensor. The dimensions of the polymer melt in the air gap (a), $H_3 = 0.49$ mm, $W_3 = 21.8$ mm, $L_3 = 85$ mm, and (b) $H'_3 = 1.2$ mm, $W'_3 = 44$ mm, $L'_3 = 85$ mm. [Color figure can be viewed in the online issue, which is available at wileyonlinelibrary.com.]

rates $\dot{\gamma} \gtrsim 30 \ \ s^{-1}$) and for PE-MA (at all shear rates examined, $\dot{\gamma} \geq 0.1 \ \ s^{-1}$). We also measured strong extensional thickening for PE-MA as shown in Figure 1b.

The extent of molecular alignment and deformation typically increases with *Wi*, and also increases as a function of total strain, e.g., as observed by various studies on morphologies associated with shear-induced crystallization.[42–44] For example, Somani et al.[42] studied molecular orientation/extension of a polymer melt (isotactic polypropylene) in response to shear flow. They found that molecular orientation/extension increased with *Wi* for fixed strain, but also increased with strain at fixed *Wi*. Thus, a combination of strong flow (high *Wi*), and sufficient duration of flow (high strain), causes alignment and deformation of chains away from the equilibrium conformation. We next calculate *Wi* and the strains involved in the flow processing studied here.

The deformations in the air gap are negligible for the observed reaction rates here, because any significant deformation occurs close to the chill rolls, and at this point the reaction is immediately quenched due to a sudden temperature drop. In our setup (Figure 3) compression/extension deformation occurs both within the die (length L_1 and L_2) and across the air gap (length L_3). The air gap length L_3 does influence the total *reaction time* after the die exit, due to variable take-up speed at the rolls. Although we believe that deformations in the air gap are negligible, we still report them to fully describe the kinematics.

For the coextrusion process in our study, we calculated the deformation rates along all coordinate axes with the different dies to demonstrate different degrees of chain extension. The same assumptions are applied as in our previous article,[5] i.e., perfect slip boundary conditions and plug flow. The results are plotted in Figure 12. Within the noncompressive die (Figure 12b) the compression rate is zero $\dot{\varepsilon}_{zz} = 0$, but the spanwise expansion causes a maximum deformation rate at the beginning of the die $\dot{\varepsilon}_{yy} = -\dot{\varepsilon}_{xx} = 0.16 \ \ s^{-1}$ with total spanwise strain $\varepsilon_{yy} = \ln(W'_2/W'_1) = 1.16$. Outside of the noncompressive die, in the air gap, the deformation rate remains low until just before the rolls. For the maximum take-up speed (185 cm/min), the maximum rate at the chill rolls is $\dot{\varepsilon}_{zz} = -1.07 \ \ s^{-1}$, with maximum compressive strain, $\varepsilon_{zz} = \ln(H'_3/H'_2) = -2.34$ at which point the reaction is quenched.

Inside the compressive die, the compression rate is nonzero and large, and there is time for the reaction to develop through the air gap. At the die exit the maximum rate is $\dot{\varepsilon}_{zz} = -4.9 \ \ s^{-1}$ with total compressive strain $\varepsilon_{zz} = \ln(H_2/H_1) = -2.34$. After exiting the die, the bilayer experiences much smaller deformation throughout the air gap and at the chill rolls the rate abruptly rises at which point the reaction is quenched. For the maximum take-up speed (185 cm/min), the maximum strain rate at the chill rolls is about $\dot{\varepsilon}_{zz} = -0.89 \ \ s^{-1}$ with maximum air gap strain $\varepsilon_{zz} = -0.9$.

The rates in the compressive die are in the shear-thinning region of PE-MA (Figure 1a), and we, therefore, expect chain extension/orientation under these conditions. To calculate a specific *Wi*, we estimated the longest relaxation time λ. From the oscillatory data in Figure 2, we obtained $\lambda = 17$ s as the longest relaxation time for PE-MA by fitting a generalized Maxwell model.[23] The maximum *Wi* in the compressive die is then determined to be $Wi = \lambda|\dot{\varepsilon}_{zz}| = 83.3$ (due to compression normal to the interface). For the noncompressive die, $Wi = 0$ due to compression normal to the interface, and $Wi = 2.7$ due to spanwise extension. The high *Wi* implies chain stretching in the compressive die during melt processing. For the noncompressive die, polymer chains stayed closer to their equilibrium configuration along the entire process.

As previously discussed, there was significant stretching of polymer chains when the reactive bilayers were extruded through the compressive die. It has been shown that stretching a polymer chain can accelerate chemical reactions of its monomer units by many orders of magnitude.[41,45–47] Although it is uncertain how stretching polymer chains could influence interfacial reaction rate, we speculate that functional polymers are driven into the interface and stretched by flow, increasing the collision possibility of functional groups.

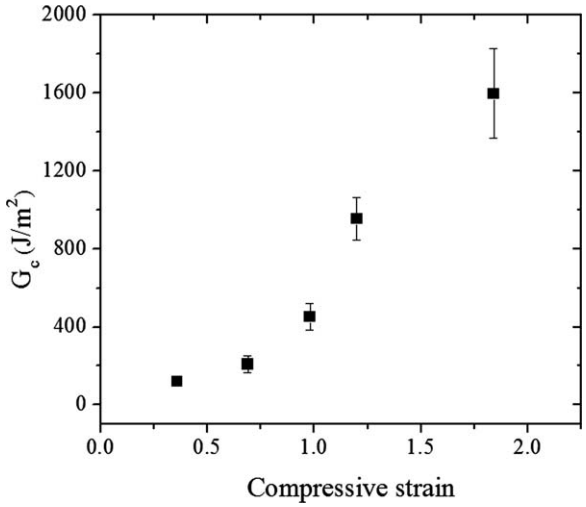

Figure 13. G_c vs. compressive strain for lamination between PE-MA and nylon 6 annealed for 10 s at 230°C.

The interface between two immiscible polymers plays the role of diffusion barrier, hindering the diffusion of both reactive polymer chains to the interface for chemical reactions. Rafailovich et al. [48] found that the diffusion rate is one-order of magnitude slower near an interface compared with in the bulk. We speculate that compressive flow, especially confined compressive flow which produces compressive stress at the interface, helps to extend chains and also force reactive species to an interface, increasing interfacial thickness and, thus, the concentration of reactive species in the interface. In addition, the interaction between MA groups with the nylon backbone or between NH_2 with PE is repulsive. Compressive flow opposes this repulsive force and may facilitate reaction. Moreover, we speculate that the polar functional groups attached to the nonpolar hydrocarbon backbones have the tendency to aggregate. Flow may facilitate release of the functional groups from aggregated cages and expose them to interfacial reaction.

To further test the hypothesis that compressive deformation normal to the interface accelerates interfacial reaction, we repeated some lamination tests with more compressive flow. Table 1 and Figure 13 show that as the magnitude of compressive Hencky strain increased, the adhesion strength increased dramatically within only 10 s annealing time. Thus, when a larger compressive strain was applied normal to the interface, more copolymers were generated at the interface. The G_c value at the highest compressive strain in lamination, $G_c = 1598$ J/m^2 at $\varepsilon_{zz} = -1.84$ (with 10 s of annealing time), is very similar to that for the compressive coextrusion die with a reaction time of 10 s, $G_c = 1500$ J/m^2 with maximum strain $\varepsilon_{zz} = -2.34$. This indicates that lamination with high compressive strain can generate a similar two-orders of magnitude increase in reaction rate over lamination or coextrusion without compression. We therefore observe that the interfacial reaction rate increases as a function of both increasing compressive flow strength (increasing *Wi*) (Table 1, Figures 9–11), and increasing strain at constant compressive stress (Figure 13). These trends are consistent with the idea of flow-induced chain extension that increases as a function of both flow strength (*Wi*) and total strain.

Conclusion

Coupling reaction occurred during coextrusion and lamination of a nylon 6/PE-MA bilayer. It is striking that holding all other parameters constant, the reaction rate during coextrusion through the *compressive* die was almost two-orders of magnitude larger than that through the *noncompressive* die. The reaction rate through the noncompressive die was found close to that of quiescent lamination. Lamination coupled with large compressive strain was also able to accelerate reaction similar to the compressive die.

We directly measured the formed copolymer density at the interface because it is the copolymer density that reflects reaction rate and determines adhesion strength. This enabled us to directly calculate reaction rates instead of inferring them from adhesion strength,[5] even though both ways lead to the same conclusion: *compressive* flow accelerates interfacial coupling reactions, hence, stronger adhesion. We showed that adhesion follows the scaling found with block copolymer coverage for glassy polymers: linear at low coverage and $G_c \propto \sum^2$ at higher coverage even for our semicrystalline polymers with graft copolymers at the interface. In our previous article,[5] we coupled amine grafted polyethylene with polyurethane and found that compressive flow also accelerates interfacial reaction but only 10-fold. The faster reactivity in this work is most likely due to the higher temperature and inherently faster reactivity of primary amine groups on the ends of nylon 6 chains with the anhydride grafts on PE.

For the coextrusion experiments reported here, the interface was under compression/extension conditions and in the absence of shear or mixing. We compared the degree of chain extension by calculating the Weissenberg number. We calculated the deformation rates along all coordinate axes during the coextrusion process with different dies. For the noncompressive die, the compressive strain rate is zero ($Wi = \lambda\dot{\varepsilon}_{zz} = 0$) although the spanwise strain rate gives $Wi = 2.7$ with spanwise strain $\varepsilon_{yy} = 1.16$. In contrast, in the compression die, the compressive strain rate generates $Wi = 83.3$ with compressive strain $\varepsilon_{zz} = -2.34$. A direct result of large deformation rate was that polymer chains were stretched significantly in the compressive die, whereas in the noncompressive die they stayed closer to the equilibrium conformation. Compressive flow with compressive stress may also increase the thickness of the interfacial region and reduce aggregation between polar functional groups. The coupling reaction rate was also accelerated for simple lamination when compressive flow and compressive stress were applied normal to the interface.

Beyond its scientific significance, this work illustrates why coextusion is so successful for producing multilayer products within a very short residence time. Increasing the strength of compressive flow normal to the interface can build up interfacial adhesion much faster, independent of other processing variables. Taking advantage of flow conditions during polymer processing creates opportunities for designing new reactions, products and materials.

Acknowledgements

This work was supported by The Dow Chemical Co. Aaron Hedegaard provided the extensional viscosity data. Parts of this work were carried out in the Characterization Facility, University of Minnesota, which receives partial support from NSF through the MRSEC program.

Literature Cited

1. Warden RB, Amundson NR. Stability and control of addition polymerization reactions: A theoretical study. *Chem Eng Sci.* 1962;17(10):725–734.
2. Zeman R, Amundson NR. Continuous models for polymerization. *AIChE J*. 1963;9(3):297–302.
3. Goldstein RP, Amundson NR. An analysis of chemical reactor stability and control-Xa: Polymerization models in two immiscible phases in physical equilibrium. *Chem Eng Sci*. 1965;20(3):195.
4. Sundararaj U, Macosko CW. Drop breakup and coalescence in polymer blends: The effects of concentration and compatibilization. *Macromolecules*. 1995;28(8):2647.
5. Song J, Ewoldt RH, Hu W, Silvis HC, Macosko CW. Flow accelerates adhesion between functional polyethylene and polyurethane. *AIChE J*. 2011;57(12):3496–3506.
6. Creton C, Kramer EJ, Brown HR, Hui CY. Adhesion and fracture of interfaces between immiscible polymers: from the molecular to the continuum scale. *Adv Polym Sci*. 2001;156:53–136.
7. D. R. Paul, Bucknall CB. *Polymer Blends: Formulation*. Vol 1. New York: Wiley-Interscience; 2000.
8. Kobayashi S, Song J, Silvis HC, Macosko CW, Hillmyer MA. Amino-functionalized polyethylene for enhancing the adhesion between polyolefins and polyurethanes. *Ind Eng Chem Res*. 2011;50(6):3274–3279.
9. Song J, Thurber CM, Kobayashi S, Baker AM, Macosko CW, Silvis HC. Blends of polyolefin/PMMA for improved scratch resistance, adhesion and compatibility. *Polymer*. 2012;53(16):3636–3641.

10. Orr CA, Cernohous JJ, Guegan P, Hirao A, Jeon HK, Macosko CW. Homogeneous reactive coupling of terminally functional polymers *Polymer*. 2001;42(19):8171–8178.
11. Jeon HK, Macosko CW, Moon B, Hoye TR, Yin Z. Coupling reactions of end- vs mid-functional polymers. *Macromolecules*. 2004;37(7):2563–2671.
12. Schulze JS, Cernohous JJ, Hirao A, Lodge TP, Macosko CW. Reaction kinetics of end-functionalized chains at a polystyrene/poly (methyl methacrylate) interface. *Macromolecules*. 2000;33(4):1191.
13. Zhang J, Lodge TP, Macosko CW. Interfacial morphology development during PS/PMMA reactive coupling. *Macromolecules*. 2005;38:6583.
14. Song J, Bringuier A, Kobayashi S, Baker AM, Macosko CW. Adhesion between polyethylenes and different types of polypropylenes. *Polym J*. 2012;44:939–945.
15. Su YY, Khomami B. Interfacial stability of mulitlayer viscoelastic fluids in slit and coverging channel die geometries. *J Rheol*. 1992;36(2):357–387.
16. Wang L, Shogren RL, Carriere C. Preparation and properties of thermoplastic starch-polyester laminate sheets by coextrusion. *Polym Eng Sci,*. 2000;40(2):499–506.
17. Martin O, Schwach E, Averous L, Couturier Y. Properties of biodegradable multilayer films based on plasticized wheat starch. *Starch Starke*. 2001;53(8):372–380.
18. Lee P, Park HE, Morse DC, Macosko CW. Polymer–polymer interfacial slip in multilayered films. *J Rheol*. 2009;53(4):893.
19. Zhao R, Macosko CW. Polymer–polymer mutual diffusion via rheology of coextruded multilayers. *AIChE J*. 2007;53(4):978–985.
20. Zhang J, Ji S, Song J, Lodge TP, Macosko CW. Flow accelerates interfacial coupling reactions. *Macromolecules*. 2010;43(18):7617–7624.
21. Zhao R, Macosko CW. Slip at polymer–polymer interfaces: rheological measurements on coextruded multilayers. *J Rheol*. 2002;46(1):145–167.
22. Macosko CW, Jeon HK, Hoye TR. Reactions at polymer–polymer interfaces for blend compatibilization. *Prog Polym Sci*. 2005;30:939.
23. Macosko CW. *Rheology-Principles, Measurements, and Applications*. New York: Wiley; 1994.
24. Lee PC, Park HE, Morse DC, Macosko CW. Polymer–polymer interfacial slip in multilayered films. *J. Rheol*. 2009;53(4):893–915.
25. Song J. Interfacial Coupling between Immiscible Polymers: Flow Accelerates Reaction and Improves Adhesion *[PhD thesis]*. Minneapolis, MN: University of Minnesota; 2012.
26. Creton C, Kramer EJ, Hui CY, Brown HR. Failure mechanisms of polymer interfaces reinforced with block copolymers. *Macromolecules*. 1992;25(12):3075–3088.
27. Boucher E, Folkers JP, Creton C, Hervet H, Leger L. Enhanced adhesion between polypropylene and polyamide-6: Role of interfacial nucleation of the beta-crystalline form of polypropylene. *Macromolecules*. 1997;30(7):2102–2109.
28. Kanninen MF. An augmented double cantilever beam model for studying crack propagation and arrest *Intl J Frac*. 1973;9(1):83–92.
29. Boucher E, Folkers JP, Hervet H, Leger L, Creton C. Effects of the formation of copolymer on the interfacial adhesion between semicrystalline polymers. *Macromolecules*. 1996;29(2):774–782.
30. Wagner CD, Davis LE, Zeller MW, Taylor JA, Raymond RH, Gale LH. Empirical atomic sensitivity factors for quantitative analysis by electron spectroscopy for chemical analysis. *Surf Interface Anal*. 1981;3:211.
31. Cumpson PJ, Seah MP. Elastic scattering corrections in AES and XPS.2. Estimating attenuation lengths and conditions required for their valid use in overlayer/substrate experiments. *Surf Interface Anal*. 1997;25(6):430–446.
32. Boucher E, Folker JP, Creton C, Hervet H, Leger L. Enhanced adhesion between polypropylene and polyamide-6: role of interfacial nucleation of the β-crystalline form of polypropylene. *Macromolecules*. 1997;30(7):2102–2109.
33. Dai C, Kramer EJ, Washiyama J, Hui C. Fracture toughness of polymer interface reinforced with diblock copolymer: effect of homopolymer molecular weight. *Macromolecules*. 1996;29(23):7536–7543.
34. Brown HR. A molecular interpretation of the toughness of glassy polymers. *Macromolecules*. 1991;24(10):2752–2756.
35. Sha Y, Hui CY, Ruina A, Kramer EJ. Continuum and discrete modeling of craze failure at a crack-tip in a glassy polymer. *Macromolecules*. 1995;28(7):2450–2459.
36. Steinfeld JI, Francisco JS, Hase WL. *Chemical Kinetics and Dynamics*. *2nd ed*. Upper Saddle River, New Jersey: Prentice Hall; 1998.
37. Seo Y, Ninh TH. Enhanced interfacial adhesion between polypropylene and nylon 6 by in situ reactive compatibilization. *Polymer*. 2004;45(25):8573–8581.
38. Seo Y, Kang T. Interfacial adhesion between semi-crystalline polymers (polypropylene and nylon-6): in situ compatibilized interface and fracture mechanism. *Compos Interface*. 2006;13(7):605–621.
39. Chaffin KA, Knutsen JS, Brant P, Bates FS. High-strength welds in metallocene polypropylene/polyethylene laminates. *Science*. 2000;288(5474):2187–2190.
40. Kumaraswamy G, Kornfield JA, Yeh FJ, Hsiao BS. Shear-enhanced crystallization in isotactic polypropylene. 3. Evidence for a kinetic pathway to nucleation. *Macromolecules*. 2002;35(5):1762–1769.
41. Ribas-Arino J, Marx D. Covalent mechanochemistry: Theoretical concepts and computational tools with applications to molecular nanomechanics. *Chem Rev*. 2012;112(10):5412–5487.
42. Somani RH, Yang L, Hsiao BS, Sun T, Pogodina NV, Lustiger A. Shear-induced molecular orientation and crystallization in isotactic polypropylene: Effects of the deformation rate and strain. *Macromolecules*. 2005;38(4):1244–1255.
43. Chellamuthu M, Arora D, Winter HH, Rothstein JP. Extensional flow-induced crystallization of isotactic poly-1-butene using a filament stretching rheometer. *J Rheol*. 2011;55(4):901–920.
44. Elmoumni A, Winter HH. Large strain requirements for shear-induced crystallization of isotactic polypropylene. *Rheol Acta*. 2006;45(6):793–801.
45. Lenhardt JM, Ong MT, Choe R, Evenhuis CR, Martinez TJ, Craig SL. Trapping a diradical transition state by mechanochemical polymer extension. *Science*. 2010;329(5995):1057–1060.
46. Hickenboth CR, Moore JS, White SR, Sottos NR, Baudry J, Wilson SR. Biasing reaction pathways with mechanical force. *Nature*. 2007;446(7134):423–427.
47. Wiggins KM, Bielawski CW. A mechanochemical approach to deracemization. *Angew Chem Int Ed*. 2012;51(7):1640–1643.
48. Zheng X, Rafailovich MH, Sokolov J et al. Long-range effects on polymer diffusion induced by a bounding interface. *Phys Rev Lett*. 1997;79(2):241–244.

Appendix: Calculation of Deformation Rates in Coextrusion Process

Given an extrusion die with changing rectangular cross section, with "slipping" plug flow (as in Song et al.[5]), we calculated:

a. The deformation rate tensor **2D**, for the possible compression/extension in the coordinate directions;
b. The deformation-rate magnitude $\dot{\gamma}=|II_{2D}|^{1/2}$, related to the second invariant of the deformation-rate tensor. (Another invariant $III_{2D}=\det[\mathbf{2D}]$, was not used because this measure has the problem of being zero for planar elongation, which is possible in compressive coextrusion).

We neglect shear components and use the notation

$$\dot{\varepsilon}_{xx}=dv_x/dx$$
$$\dot{\varepsilon}_{yy}=dv_y/dy$$
$$\dot{\varepsilon}_{zz}=dv_z/dz$$

so that the deformation rate tensor takes the form

$$\mathbf{2D}=\nabla\mathbf{v}+(\nabla\mathbf{v})^T=\begin{bmatrix}2\dot{\varepsilon}_{xx} & 0 & 0\\ 0 & 2\dot{\varepsilon}_{yy} & 0\\ 0 & 0 & 2\dot{\varepsilon}_{zz}\end{bmatrix}$$

Note that incompressible flow requires $\nabla\cdot\mathbf{v}=0$, and, therefore $\dot{\varepsilon}_{xx}+\dot{\varepsilon}_{yy}+\dot{\varepsilon}_{zz}=0$ which allows us to rewrite one of the components in terms of the others. It is most convenient to rewrite the downstream component as $\dot{\varepsilon}_{xx}=-\dot{\varepsilon}_{yy}-\dot{\varepsilon}_{zz}$ With this, the deformation rate tensor can be rewritten as

$$\mathbf{2D}=2\begin{bmatrix}-\dot{\varepsilon}_{yy}-\dot{\varepsilon}_{zz} & 0 & 0\\ 0 & \dot{\varepsilon}_{yy} & 0\\ 0 & 0 & \dot{\varepsilon}_{zz}\end{bmatrix}$$

and only two unknowns must be solved. The y- and z-directions are confined, and deformation rates can be found following Song et al.[5] In the spanwise direction

$$\dot{\varepsilon}_{yy}=\frac{dv_y}{dy}=v_x\left(\frac{1}{W}\frac{dW}{dx}\right)$$
$$=\frac{Q}{HW}\left(\frac{1}{W}\frac{dW}{dx}\right)$$

and in the direction normal to the interface

$$\dot{\varepsilon}_{zz}=\frac{dv_z}{dz}=v_x\left(\frac{1}{H}\frac{dH}{dx}\right)$$
$$=\frac{Q}{HW}\left(\frac{1}{H}\frac{dH}{dx}\right)$$

To solve for the magnitude of the deformation rate tensor $\dot{\gamma}=|II_{\mathbf{2D}}|^{1/2}$, we recall the definition of $\boldsymbol{II}_{\mathbf{2D}}$ and

$$II_{\mathbf{2D}}=\frac{1}{2}\left[(tr[\mathbf{2D}])^2-tr\left([\mathbf{2D}]^2\right)\right]$$
$$=4\left[\dot{\varepsilon}_{xx}\dot{\varepsilon}_{yy}+\dot{\varepsilon}_{xx}\dot{\varepsilon}_{zz}+\dot{\varepsilon}_{yy}\dot{\varepsilon}_{zz}\right]$$

Using the incompressibility result $\dot{\varepsilon}_{xx}=-\dot{\varepsilon}_{yy}-\dot{\varepsilon}_{zz}$ then gives

$$II_{\mathbf{2D}}=-4\left[\dot{\varepsilon}_{yy}{}^2+\dot{\varepsilon}_{yy}\dot{\varepsilon}_{zz}+\dot{\varepsilon}_{zz}{}^2\right]$$

The previous results for $\dot{\varepsilon}_{yy}$ and $\dot{\varepsilon}_{zz}$ can be used to give the final result

$$\dot{\gamma}=|II_{\mathbf{2D}}|^{1/2}=2\frac{Q}{H(x)W(x)}\left[\left(\frac{1}{W(x)}\frac{dW}{dx}\right)^2+\left(\frac{1}{H(x)}\frac{dH}{dx}\right)^2+\left(\frac{1}{W(x)}\frac{dW}{dx}\right)\left(\frac{1}{H(x)}\frac{dH}{dx}\right)\right]^{1/2}$$

We use $\dot{\gamma}=|II_{\mathbf{2D}}|^{1/2}$ to represent the effective strain-rate magnitude. The term in brackets will always be positive, although the cross term arising from the product $\dot{\varepsilon}_{yy}\dot{\varepsilon}_{zz}$ may be negative. In such a case where $\dot{\varepsilon}_{yy}\dot{\varepsilon}_{zz}<0$ it may be possible for the magnitude of $\dot{\gamma}$ to be smaller than the magnitude of the dominant extensional component (e.g., in Figure 12).

Manuscript received Oct. 11, 2012; revision received Dec. 24, 2012, and final revision received Mar. 12, 2013.